9-2020

BK Potassium Currents Contribute Differently to Action Potential Waveform and Firing Rate as Rat Hippocampal Neurons Mature in The First Postnatal Week

Michael Hunsberger

Michelle Mynlieff

Journal of Neurophysiology, Vol. 124, No. 3 (September 2020): 703-714. DOI.

BK Potassium Currents Contribute Differently to Action Potential Waveform and Firing Rate as Rat Hippocampal Neurons Mature in The First Postnatal Week

Michael S. Hunsberger
Department of Biological Sciences, Marquette University, Milwaukee, Wisconsin
Michelle Mynlieff
Department of Biological Sciences, Marquette University, Milwaukee, Wisconsin

Abstract

The large-conductance calcium-activated potassium (BK) channel is a critical regulator of neuronal action potential firing and follows two distinct trends in early postnatal development: an increase in total expression

and a shift from the faster activating STREX isoform to the slower ZERO isoform. We analyzed the functional consequences of developmental trends in BK channel expression in hippocampal neurons isolated from neonatal rats aged 1 to 7 days. Following overnight cultures, action potentials and currents were recorded using whole cell patch-clamp electrophysiology. These neurons undergo a steady increase in excitability during this time, and the effect of blockade of BK channel activity with 100 nM iberiotoxin changes as the neurons mature. BK currents contribute significantly more to total potassium current and single action potentials in neurons of 1-day old rats (with BK blockade extending action potential duration by 0.46 ± 0.12 ms) than in those of 7-day old rats (with BK blockade extending action potential duration by 0.17 ± 0.05 ms). BK currents contribute consistently to maintain firing rates in neurons of 1-day old rats throughout extended action potential firing; BK blockade evenly depresses firing frequency across action potential trains. In neurons from 7-day old rats, BK blockade initially increases firing frequency and then progressively decreases frequency as firing continues, ultimately depressing neuronal firing rates to a greater extent than in the neurons from 1-day-old animals. These results are consistent with a transition from low expression of a fast-activating BK isoform (STREX) to high expression of a slower activating isoform (ZERO).

NEW & NOTEWORTHY This work describes the early developmental trends of large-conductance calcium-activated potassium (BK) channel activity. Early developmental trends in expression of BK channels, both total expression and relative isoform expression, have been previously reported, but little work describes the effect of these changes in expression patterns on excitability. Here, we show that early changes in BK channel expression patterns lead to changes in the role of BK channels in determining the action potential waveform and neuronal excitability.

INTRODUCTION

The brain undergoes major developmental changes in excitability from infancy to adulthood. These include reorganization and establishment of circuits (Cline 2001; Gómez-Di Cesare et al. 1997; Huttenlocher and Dabholkar 1997), development of GABAergic and glutamatergic neurotransmitter systems (Dzhala and Staley 2003; Kumar et al. 2002; Szczurowska and Mareš 2013), and changes in the intrinsic excitability of cells resulting from establishment of mature patterns of voltage-gated ion channel expression (Gao and Ziskind-Conhaim 1998; Picken Bahrey and Moody 2003). Changes in intrinsic excitability are reflected in changes in the action potential waveform. Data from cortical pyramidal neurons, neocortical and cortical interneurons, and spinal motor neurons show that the neuronal action potential waveforms transition from longer lasting, low-amplitude spikes in immature neurons to high-amplitude, brief spikes accompanied by faster firing rates in mature neurons (Gao and Ziskind-Conhaim 1998; Goldberg et al. 2011; Kinnischtzke et al. 2012; McCormick and Prince 1987; Picken Bahrey and Moody 2003).

The large-conductance high-voltage and calcium-activated potassium channel (BK channel, Slo1, Maxi-K, Kcnma1) plays a central role in neuronal excitability and is also implicated in developmental changes in excitability. The BK channel is expressed along the axon and at presynaptic terminals, positioning it to regulate the frequency of action potential firing and neurotransmitter release (Gu et al. 2007; Jaffe et al. 2011; Misonou et al. 2006). BK channel expression patterns change through early development suggesting that its role in regulating excitability may be developmentally dependent. There is a several fold increase in total BK mRNA levels from late embryonic development to the first postnatal week in rodents; at the same time the predominant isoform shifts from STREX to the ZERO isoform (MacDonald et al. 2006). The STREX (STRess hormone-regulated EXon) isoform contains a 57 amino acid insert in the intracellular calcium sensing domain that confers higher calcium sensitivity and thus, requires lower calcium concentrations to shift the activation voltage to physiologically relevant potentials (Chen et al. 2005; Xie and McCobb 1998). Currents of the STREX isoform exhibit faster activation than those of the insertless ZERO isoform. In addition, the STREX insert changes

the response of BK channels to phosphorylation so that phosphorylation by protein kinase A (PKA) causes inhibition of current in contrast to the typical increase in BK current seen in ZERO. In ZERO, phosphorylation by protein kinase C (PKC) leads to a decrease in BK current whereas the STREX isoform is insensitive to PKC phosphorylation (Zhou et al. 2010, 2012).

While the developmental changes in BK mRNA levels have been described, investigation into the effects these changes have on neuronal properties and excitability is needed. The changes in BK channel expression and isoform characteristics suggest that the role of BK channels in modulating the action potential kinetics and firing rate changes as the nervous system matures. In the present study we used hippocampal neurons isolated from rats aged 1 to 7 days to determine how excitability and the role of BK channels in this population of neurons change during this time as it is a period in which there are rapid changes in BK expression levels and isoforms.

We found, in agreement with earlier findings in cortical pyramidal neurons, cortical interneurons, and spinal neurons (Gao and Ziskind-Conhaim 1998; Goldberg et al. 2011; Kinnischtzke et al. 2012; McCormick and Prince 1987), that hippocampal neurons become more excitable through early development as evidenced by greater firing rates and a transition from slow, low amplitude action potentials to fast, higher amplitude action potentials. Through this period, BK channel expression greatly increases and the effect of blocking BK channel activity changes. BK channel blockade has a greater effect on the duration of single action potentials at postnatal *day 1* than at postnatal *day 7* despite large increases in total BK channel expression as development progresses. BK channel blockade also depresses firing rates to a greater extent at the onset of successive action potential firing in neurons from postnatal *day 1* rats than in neurons from postnatal *day 7* rats but has a greater effect in neurons from 7-day-old rats as successive action potential firing continues.

MATERIALS AND METHODS

Laboratory animals.

All animal protocols were approved by the Marquette University Institutional Animal Care and Use Committee according to the guidelines set forth by the National Research Council in the *Guide for Care and Use of Laboratory Animals*. Sasco Sprague-Dawley rats (Charles River; Wilmington, MA) were housed and bred at Marquette University. Pups were removed from mothers just before tissue isolation.

Isolation and culturing of hippocampal neurons.

Acute primary cultures of hippocampal neurons were obtained as previously described (Mynlieff 1997). Briefly, the superior regions of the hippocampi were dissected from postnatal *day 1* through *7* (P1–P7) rat pups in cold, oxygenated rodent Ringer's solution (146 mM NaCl, 5 mM KCl, 2 mM $CaCl_2$, 1 mM $MgCl_2$, 10 mM HEPES, and 11 mM d-glucose, adjusted to pH 7.4 with NaOH). Tissue was incubated in piperazine-*N*-*N*'-bis-2-ethanesulfonic acid (PIPES)-buffered saline (120 mM NaCl, 5 mM KCl, 1 mM $CaCl_2$, 1 mM $MgCl_2$, 25 mM glucose, and 20 mM PIPES, adjusted to pH 7.0 with NaOH) with 0.5% trypsin type XI (Sigma-Aldrich, St. Louis, MO) and 0.01% DNase type I (Worthington, Lakewood, NJ) for 20–30 min at room temperature under oxygen. This was followed by a 60-min incubation at 35°C under continuous oxygen. Enzymatic activity was terminated by rinsing the tissue with trypsin inhibitors (1 mg/mL trypsin inhibitor type II-O: chicken egg white and 1 mg/mL bovine serum albumin; Sigma-Aldrich, St. Louis, MO) in rodent Ringer's solution. Following incubation, tissue was triturated to dissociate neurons and plated onto poly-l-lysine (30,000–70,000; Sigma-Aldrich, St. Louis, MO)-coated culture dishes with Gibco neurobasal-A culture medium (ThermoFisher Scientific, Waltham, MA) fortified with B-27 supplement, 0.5 mM glutamine, and 0.02 mg/mL gentamicin. Neurons were held in a 37°C, 5% CO_2 incubator overnight to allow for reinsertion of membrane proteins while minimizing in vitro developmental changes.

Slice preparation.

Brains of rats aged P4–P5 and P7–P8 were removed and immediately immersed in ice cold, oxygenated high-sucrose artificial cerebral spinal fluid (aCSF; 129 mM sucrose, 3 mM KCl, 1.4 mM $CaCl_2$, 1.2 mM $MgSO_4$, 10 mM d-glucose, 25 mM HEPES, and 0.4 mM l-ascorbic acid, pH adjusted to 7.4 with NaOH). Coronal slices (200–300 µm) were obtained using a Vibroslice (Campden instruments, Lafayette, IN). Slices containing sections of the hippocampus were reserved in room temperature, oxygenated aCSF (129 NaCl, 3 mM KCl, 1.4 mM $CaCl_2$, 1.2 mM $MgSO_4$, 10 mM d-glucose, 25 mM HEPES, and 0.4 mM l-ascorbic acid, pH adjusted to 7.4 with NaOH; Fridén et al. 2009) for a minimum of 1 h before recording.

Electrophysiology-cultured neurons.

Recordings were taken from cultured neurons the day after isolation to minimize the outgrowth of processes at room temperature. Both currents and potentials were obtained by whole cell patch-clamp recording with a Dagan 3900A patch-clamp amplifier (Dagan Corporation, Minneapolis, MN), Axon Digidata 1322A 16-bit data acquisition system, and pClamp 10.4 data acquisition software (Molecular Devices, San Jose, CA). Thick-walled borosilicate pipettes (≈4–8 MΩ) were filled with internal solution (140 mM K-gluconate, 0.5 mM $CaCl_2$, 2 mM $MgCl_2$ 1 mM EGTA, 2 mM ATP-Na_2, 0.2 mM GTP-Na_2, and 10 mM HEPES, adjusted to pH of 7.2–7.4 with KOH). The free calcium concentration using this intracellular solution was estimated to be 130 nM at rest using the Maxchelator Ca/Mg/ATP/EGTA Calculator v2.2b (https://somapp.ucdmc.ucdavis.edu/pharmacology/bers/maxchelator/CaMgATPEGTA-NIST-Plot.htm). Cells were placed in an extracellular recording solution (115 mM NaCl, 25 mM $NaHCO_3$, 2.5 mM KCl, 2 mM $CaCl_2$, 1 mM $MgCl_2$, 10 mM glucose, and 10 mM HEPES, adjusted to pH of 7.4 with NaOH).

Single action potentials and trains of action potentials were measured in current-clamp mode. The Dagan 3900A is a bath-driven patch-clamp amplifier, which is rapid enough to avoid the errors in current clamp mode seen with other non-bath driven amplifiers (Magistretti et al. 1996). The membrane potential and membrane properties were recorded upon initial break-in and then adjusted to between −65 and −70 mV by current injection to allow for comparisons between cells as the afterhyperpolarization (AHP) and firing properties are dependent on the resting membrane potential. Single action potentials were elicited by a 0.1-ms, 8-nA current injection, which was sufficient to produce action potentials consistently in all cells. Action potential trains were elicited by 100-ms and 1-s depolarizing current injections ranging from 10 to 200 pA until a maximum number of action potentials was evoked. Data was digitized at a rate of 20 kHz with a 10-kHz lowpass filter. All membrane potentials reported have been adjusted postrecording to account for the liquid junction potential (15.4 mV in cultured cell recordings, 17.2 in slice recordings). Passive membrane properties were measured using the membrane test tool in PClamp 10. Data were not included in the analysis from cells for which stable membrane properties were not attainable or if the action potential response or currents (below) were not relatively stable over time.

Voltage-clamp recording in whole cell mode was utilized to measure potassium currents in cultured neurons at room temperature. For these experiments, 1 µM tetrodotoxin (Alomone Labs, Jerusalem, Israel) was added to the bath solution to block voltage-dependent sodium currents. Potassium currents were evoked by 100-ms depolarizations from −50 mV to + 50 mV from a holding potential of −90 mV.

To assess the contribution of BK channels to action potentials and potassium currents in cultured neurons, 100 nM Iberiotoxin (Alomone Labs, Jerusalem, Israel) was administered using a U-tube drug delivery system consisting of PE-10 polyethylene tubing with a single perforation to allow transient, focal drug application.

Electrophysiology-acute brain slices.

Acute slice recordings were performed using the same equipment and protocols described above. The internal pipette solution was the same as used in cultured neurons, but the external solution was oxygenated aCSF to maintain viability. Slices were constantly perfused in oxygenated, room temperature aCSF at a rate of 2–4 mL/m in an open bath chamber.

Drug preparation.

Iberiotoxin (IbTx; Alomone Labs, Jerusalem, Israel) was dissolved to a 1-mM intermediate stock in extracellular recording solution and stored at −20°C in multiple aliquots to minimize freeze-thaw cycles. One millimolar of IbTx stock was thawed and added to the extracellular recording solution the same day it was used for recording to prepare a 100-nM working solution (K_i = 250 pM to 1 nM; Galvez et al. 1990; Koschak et al. 1997).

Data analysis.

Action potential durations were calculated as the time interval between the rising and falling phase at one-half of the spike amplitude. Fast afterhyperpolarization (fAHP) magnitude was measured as the lowest voltage attained during hyperpolarization subtracted from the resting membrane potential recorded before the stimulus used to induce the action potential. To calculate the effect of IbTx on action potential duration, fAHP, and the maximum number of action potential evoked in 100 ms, the difference between the value measured from the IbTx-treated trace and the average value measured from one untreated trace before and one after washout of IbTx was used to account for potential confounding effects of prolonged patching and electrical stimulation. Instantaneous frequencies were calculated as the inverse of the peak-to-peak time interval between two successive action potentials. For voltage camp recordings, the effect of the IbTx was calculated as the difference between the IbTx-treated trace and the mean of two traces collected before IbTx application and two collected after IbTx washout.

All statistical tests were performed using SigmaPlot 14 (Systat Software, San Jose, Ca). Much of the data collected was not normally distributed; therefore, nonparametric statistical tests were used where appropriate. All data were initially separated by sex, but ultimately the electrophysiological data were pooled as no statistical differences by sex were observed.

Western blots.

Protein was extracted from whole hippocampal homogenates from rats aged 0, 2, 4, 6, and 8 days. Hippocampi were homogenized in an ice-cold sucrose-based buffer (250 mM sucrose, 10 mM Tris, 10 mM HEPES, and 1 mM EDTA, adjusted to a final pH of 7.2 with HCl) with protease inhibitors (0.5 mg/mL Pefabloc, 1 µg/mL leupeptin, and 1 µg/mL pepstatin; Sigma-Aldrich, St. Louis, MO). This was followed by centrifugation at 3,622 *g* for 10 min at 4°C. The pellet was then discarded, and the supernatant was centrifuged at 35,000 *g* for 30 min at 4°C; the resulting pellet was saved and resuspended in fresh homogenization buffer with protease inhibitors and stored at −80°C for later use. Protein concentration was estimated by preparing samples with a BCA protein assay kit (Pierce, Rockford, IL) and measuring with a biophotometer (Eppendorf, Hamburg, Germany) at 562 nm.

Protein (1.5 µg) from each animal was denatured in NuPage lithium dodecyl sulfate (LDS) and reducing agent at 70°C for 10 min and separated on a NuPage 3–8% Tris-acetate Novex minigel (Invitrogen, Carlsbad, CA). Following gel electrophoresis, proteins were transferred to a polyvinylidene difluoride membrane (PVDF; 0.45-µm pore size) in NuPage transfer buffer (Invitrogen, Carlsbad, CA). Following transfer, membranes were washed in phosphate-buffered saline (PBS; 134.4 mM NaCl, 4.36 mM KCl, 10.56 mM Na_2HPO_4, 1.66 mM NaH_2PO_4, pH 7.4) and blocked for 1 h with PBS containing 0.05% TWEEN 20, 5% nonfat dry milk, and 0.1% bovine serum albumen at room temperature. Membranes were then incubated at 4°C overnight in blocking solution containing mouse-anti-BK antibodies (Genetex GTX54874; lot 821503077) at a 1:2,000 dilution and rabbit-anti-

α/β-tubulin antibodies (Cell Signaling Technology 2148S; lot 6) at a 1:4,000 dilution. Following decoration with primary antibodies, membranes were washed in PBS with 0.05% Tween 20 for 1 h at room temperature and decorated with goat-anti-mouse (Pierce no. 1858413; lot GC95907) and goat-anti-rabbit (Pierce no. 1858415 lot GC95095) horseradish peroxidase (HRP)-conjugated antibodies each at a 1:1,000 dilution in blocking solution for 90 min. Membranes were then washed in PBS with 0.05% Tween 20 and incubated for 5 min in SuperSignal West Dura extended signal substrate (ThermoFisher Scientific, Waltham, MA) to allow for visualization of the protein bands. Membranes were exposed to classic blue-autoradiography film (MidSci, St. Louis, MO). The integrated optical density (IOD) of the bands was measured with Labworks 4.6 imaging and analysis software (UVP, Upland, CA) to quantify relative protein content. The IOD of each BK band was divided by the IOD of the α/β-tubulin band in the same lane to control for gel loading.

RESULTS

We measured the change in BK α-subunit steady state protein expression in the hippocampi of male and female rat pups aged P0 to P8 (*n* = 3 animals per sex for each time point) to determine if protein expression follows the reported trends in mRNA expression and if there are sex differences in the protein expression (Fig. 1). There was a significant effect of sex on BK protein expression (Fig. 1*B*; two-way ANOVA $P < 0.001$) but no significant interaction of age and sex. Figure 1*C* shows the pooled results of males and females for all age groups. Consistent with previously report of rises in mRNA expression from embryonic day (E)18 to P7, we found that protein expression increases by approximately threefold from P0 to P8 (One-way ANOVA, $P < 0.001$; Holm-Sidak multiple comparisons, $P = 0.05$; MacDonald et al. 2006).

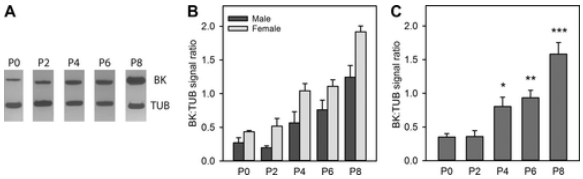

Fig. 1. Large-conductance calcium-activated potassium (BK) channel expression increases drastically during early postnatal development. *A*: representative lanes from an immunoblot of BK α-subunit and β-tubulin (Tub). *B*: bar chart comparing means ± SE ratio of BK α-subunit band intensity to β-tubulin band intensity of male and female rats at postnatal day (P)0, P2, P4, P6, and P8 (*n* = 3 for each group). BK expression is significantly higher in hippocampi from female rats overall, but no significance was detected at individual time points by pairwise comparisons ($P < 0.001$, two-way ANOVA). *C*: bar chart showing the means ± SE ratio of BK α-subunit band intensity to β-tubulin band intensity for postnatal day (P)0, P2, P4, P6, and P8 for 3 male and 3 female rats per age. *Significantly greater expression than P0; **Significantly greater expression than P0 and P2; ***Significantly greater expression than P0–P6 (one-way ANOVA, $P < 0.001$; Holm-Sidak multiple comparisons, $P = 0.05$).

Voltage and current-clamp recordings were collected from cultured hippocampal neurons of rats aged 1 to 7 days. Unlike cultures from embryonic rodents that are enriched with pyramidal neurons, these cultures have a large percentage of interneurons (Aika et al. 1994; Banker and Cowan 1979; Mynlieff 1997, 1999). For all recordings, current was injected to adjust membrane potentials to −65 to −70 mV before collecting action potential measurements to normalize the electrochemical driving force for all cells.

We found that the mean action potential amplitude increased while the duration decreased as the neurons matured (Fig. 2, *A*–*E*). The mean action potential amplitude increased from 80.96 ± 1.48 mV (*n* = 80 cells, 9 animals) in neurons isolated from 1-day-old (P1) rats to 91.65 ± 1.39 mV in neurons isolated from 7-day-old (P7) rats (*n* = 71 cells, 11 animals; one-way ANOVA on ranks, $P < 0.001$, Dunn's multiple comparisons, $P < 0.05$; Fig. 2*B*). While the amplitude significantly increased, the amplitude remained highly variable, reflecting a diverse cell

population; amplitudes ranged from 53.65 to 107.76 mV in P1 neurons to 57.71 to 108.81 mV in P7 neurons (Fig. 2*C*).

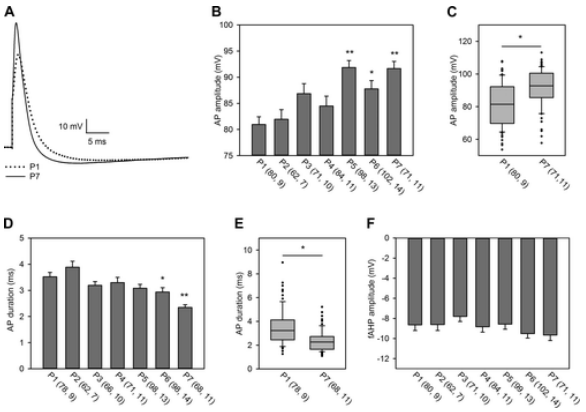

Fig. 2. Action potential (AP) waveform and firing properties change across the first postnatal week. *A*: representative traces comparing a typical action potential from a postnatal day (P)1 neuron (dotted trace) to that of a P7 neuron (solid trace). *B*: average action potential amplitudes in mV for P1 to P7 neurons. *Significant difference from P1; **significant difference from P1 and P2 (one-way ANOVA on ranks, $P < 0.001$, Dunn's multiple comparisons, $P < 0.05$). *C*: box and whisker plot of P1 and P7 action potential amplitudes is depicted to display the variability of the data. The box represents the second-third quartiles with the median indicated by the line; the whiskers represent the 10th–90th percentile. *D*: average action potential duration in ms for P1 to P7 neurons measured at half-maximal amplitude. *Significant difference from P1 and P2; **significant difference from P1 to P5 (one-way ANOVA on ranks, $P < 0.001$, Dunn's multiple comparisons $P < 0.01$). *E*: box and whisker plot of P1 and P7 action potential durations is depicted to display the variability of the data. The box represents the second-third quartiles with the median indicated by the line; the whiskers represent the 10th–90th percentile. *F*: average amplitude of fast afterhyperpolarizations (fAHP) when compared with the starting membrane potential before stimulus. For *B*, *D*, and *F*, the first number in parentheses is the number of individual neurons and the second number is the number of rats from which the neurons were obtained. The data in all bar graphs represent means ± SE.

During the same period, the mean duration, measured as the width of the action potential at half of the amplitude, decreased from 3.52 ± 0.17 ms (P1, $n = 78$ cells, 9 animals) to 2.35 ± 0.11 ms (P7, $n = 68$ cells, 11 animals; one-way ANOVA on ranks, $P < 0.001$, Dunn's multiple comparisons $P < 0.01$; Fig. 2*D*). As in the case of action potential amplitude, action potential durations were highly variable, ranging from 1.25 to 8.95 ms in P1 neurons and from 1.08 to 5.21 ms in P7 neurons (Fig. 2*E*). This sharpening of the waveform reflects developmental increases in sodium and potassium currents (Gao and Ziskind-Conhaim 1998; Picken Bahrey and Moody 2003). No significant changes were observed in the magnitude of the fast afterhyperpolarization (fAHP; Fig. 2*F*). As the neuronal population from which recordings were obtained comprises many cell types, it is possible that any age-dependent changes were obscured by the variability of the data due to cell types.

Changes in the waveform of action potentials can change the excitability of the cell as a shorter duration action potential enables a higher firing frequency (Picken Bahrey and Moody 2003). Therefore, we compared the excitability, represented by the maximal number of action potentials that could be evoked by a 100-ms depolarizing pulse, in neurons from heterogeneous hippocampal cultures across the first postnatal week. A range of pulses from 10 to 200 pA was injected into the cells, and the maximum number of action potential elicited by a single pulse is reported. P1 neurons fired on average a maximum of 2.0 ± 0.1 action potentials (n = 80 cells, 9 animals), while P7 neurons fired on average 3.3 ± 0.2 action potentials ($n = 71$ cells, 11 animals; one-way ANOVA on ranks, $P < 0.001$, Dunn's multiple comparisons, $P < 0.05$; Fig. 3). The box and whisker plot of the data from P1 and P7 demonstrates the large variability of the data set (Fig. 3*C*). In neurons obtained from P1

rats, the maximum number of action potentials elicited was 6 whereas at least 1 neuron from P7 rats fired 12 action potentials in 100 ms.

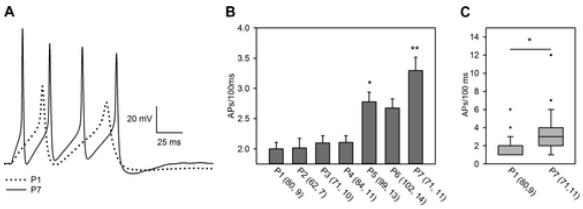

Fig. 3. Excitability of hippocampal neurons increases across the first postnatal week. *A*: representative traces comparing action potential firing in response to a 100-ms depolarizing pulse in a postnatal day (P)1 (dotted) and P7 neuron (solid). *B*: average maximal action potential (AP) firing per 100 ms for P1 to P7 neurons. *Significant difference from P1 to P2; **significant difference from P1 to 4 (one-way ANOVA on ranks, $P < 0.001$, Dunn's multiple comparisons, $P < 0.05$). The first number in parentheses is the number of individual neurons, and the second number is the number of rats from which the neurons were obtained. Data present means ± SE. *C*: box and whisker plot of P1 and P7 maximal action potentials fired per 100 ms. The box represents the second-third quartiles with the median indicated by the line; the whiskers represent the 10th–90th percentile.

The initial membrane potential upon breaking into each neuron was not significantly different in neurons obtained from P1 rats than in neurons obtained from P7 rats (Table 1). In line with reports from other cell types (Goldberg et al. 2011; Kinnischtzke et al. 2012; Picken Bahrey and Moody 2003), the mean membrane resistance of these neurons decreased from 1.93 ± 0.13 GΩ in P1 neurons ($n = 80$ cells, 9 animals) to 1.03 ± 0.11 GΩ in P7 neurons ($n = 70$ cells, 11 animals; *t* test, $P < 0.001$). The decrease in membrane resistance reflects an increase in ion channel expression with no change in the cell size as indicated by the membrane capacitance (Table 1).

Table 1. Membrane properties of P1 and P7 cultured hippocampal neurons

	P1	**P7**	***t* Test**
Resting membrane potential, mV	**−57.9 ± 1.3 (*n* = 72)**	**−56.9 ± 1.0 (*n* = 70)**	**ns**
Membrane resistance, GΩ	**1.93 ± 0.13 (*n* = 80)**	**1.03 ± 0.11 (*n* = 70)**	***P* < 0.001**
Capacitance, pF	**21.2 ± 0.7 (*n* = 72)**	**21.9 ± 0.7 (*n* = 70)**	**ns**

Data represent means ± SE. Average resting membrane potential, membrane resistance, and capacitance of cultured postnatal day (P)1 and P7 superior hippocampal neurons. Membrane resistances have been adjusted from the raw data to reflect the liquid junction potential. Statistical comparisons were made using two-sample *t* tests; ns, not significant.

We replicated the single action potential and 100-ms action potential train recordings in brain slices from male rats aged P4 to P5 and P7 to P8 to determine if the same developmental trends were present in an acute, intact system. CA1 pyramidal layer neurons in slices displayed similar age-related changes in the action potential waveform and firing rates as observed in cultured neurons (Fig. 4, *A* and *B*). The amplitude did not change significantly between these two age groups (Fig. 4*C*), but the mean action potential duration decreased from 6.89 ± 0.99 ms ($n = 9$ cells, 3 animals) to 4.5 ± 0.51 ms ($n = 18$ cells, 6 animals; Mann-Whitney rank sum test, $P < 0.02$; Fig. 4*D*). Excitability increased with P4–P5 neurons capable of firing an average maximum of 1.89 ± 0.35 action potentials ($n = 9$ cells, 3 animals) and P7–P8 neurons firing an average maximum of 3.5 ± 0.36 action potentials ($n = 18$ cells, 6 animals) in 100 ms (*t* test, $P < 0.01$; Fig. 4*E*).

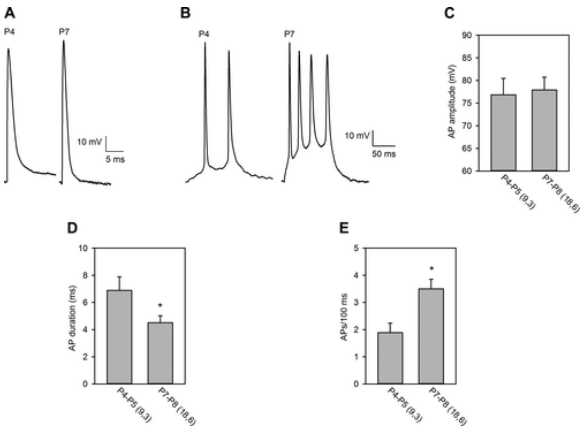

Fig. 4. Action potential and firing characteristic change as neurons mature in hippocampal slice recordings. *A*: representative traces of single action potentials recorded from CA1 hippocampal pyramidal layer neurons in slices from a postnatal day (P)4 rat (*left*) and a P7 rat (*right*). *B*: representative traces of action potential trains recorded from CA1 hippocampal pyramidal layer neurons in slices from a P4 rat (*left*) and a P7 rat (*right*). The present traces were selected from those produced by a range of inputs to show that cell's maximal response, but do not depict each cell's response to the same level of current input. The P4 neuron produced a maximum of 2 action potentials upon injection of 20 pA of current whereas the P7 neuron produced a maximum of four action potentials upon injection of 90 pA of current. *C*: average action potential (AP) amplitude in mV of P4–P5 and P7–P8 CA1 hippocampal pyramidal layer neurons in acute slice preparations. *D*: average action potential duration in ms measured at half maximal amplitude of P4–P5 and P7–P8 CA1 hippocampal pyramidal layer neurons in acute slice preparations. *Significant difference between P4–P5 and P7–P8 (Mann-Whitney rank sum test, $P < 0.05$). *E*: average maximal action potential firing per 100 ms for P4–P5 and P7–P8 CA1 hippocampal pyramidal layer neurons in acute slice preparations. *Significant difference between P4–P5 and P7–P8 (*t* test, $P < 0.01$). For *C*–*E*, the first number in parentheses is the number of individual neurons and the second number is the number of rats from which the neurons were obtained. The data in all bar graphs represent means ± SE.

As with cultured neurons, the membrane characteristics of CA1 pyramidal layer neurons were recorded. The membrane resistance and capacitance were surprisingly similar to those of cultured neurons despite the intact processes in a slice preparation. The membrane potential was more hyperpolarized than in cultured neurons, but slices required a different extracellular solution to maintain viability, so it is not a direct comparison. As in cultured neurons, neurons in slices had no significant changes in membrane potential and membrane capacitance from P4–P5 to P7–P8. In contrast with the results from cultured neurons, there was no statistically significant decrease in membrane resistance in the neurons from older rats although the data did demonstrate a trend in that direction (Table 2). This difference may be due to the abbreviated age interval and the relatively small sample size.

Table 2. Membrane properties of P4–P5 and P7–P8 CA1 hippocampal pyramidal layer neurons in acute slices

	P4–P5	**P7–P8**	***t* Test**
Resting membrane potential, mV	**−81.2 ± 2.1 (*n* = 9)**	**−78.3 ± 2.4 (*n* = 18)**	**ns**
Membrane resistance, GΩ	**1.3 ± 0.2 (*n* = 9)**	**1.0 ± 0.2 (*n* = 18)**	**ns**
Capacitance, pF	**27.0 ± 2.4 (*n* = 9)**	**24.3 ± 1.8 (*n* = 18)**	**ns**

Data represent means ± SE. Average resting membrane potential, membrane resistance, and capacitance of postnatal day (P)4–P5 and P7–P8 CA1 hippocampal pyramidal layer neurons. Membrane potentials have been

adjusted from the raw data to reflect the liquid junction potential. Statistical comparisons were made using two-sample *t* tests; ns, not significant.

To determine how BK channels contribute to action potentials across early development, we measured the effect of the selective BK channel antagonist iberiotoxin (IbTx; 100 nM) in P1–P7 neurons. The effect on duration was calculated as the difference between the action potential half-width during IbTx perfusion and the average of two control traces, one before perfusion and one after, to account for cytoplasmic washout from the recording pipette. Throughout the first postnatal week, there was less effect of IbTx on action potential duration as the neurons matured (Fig. 5, *A* and *B*). In the presence of IbTx, the duration of action potentials of P1 neurons increased by 0.63 ± 0.10 ms (n = 64 cells, 6 animals), while the duration of action potentials in P7 neurons only increased by 0.24 ± 0.08 ms (n = 45 cells, 6 animals; one-way ANOVA, P = 0.001, Dunn's multiple comparisons, P < 0.05; Fig. 5*B*). It is possible that the decrease in the effect of IbTx is the result of the decrease of the action potential duration with postnatal age rather than a result of different activity of BK channels at these two time points; the longer an action potential lasts, the longer the membrane is sufficiently depolarized for BK channels to open and IbTx will have a greater effect simply because more BK channels have opened. To investigate this possibility, we compared the effect of IbTx on action potential duration only in neurons with an initial (untreated with IbTx) action potential half-width of 2–3 ms. In this subset of P1–P2 neurons, IbTx perfusion increased mean action potential duration by 0.46 ± 0.12 ms (n = 27 cells, 12 animals) while it only increased the mean action potential durations in P6–P7 neurons by 0.17 ± 0.05 ms (n = 47 cells, 12 animals; P = 0.035; Mann-Whitney rank sum test; Fig. 5*C*). These data indicate that the age-dependent change in the effect of IbTx on action potential duration in hippocampal neurons is the result of differences in BK channel activity across the first postnatal week and not merely a consequence of changes in the overall action potential kinetics during this time.

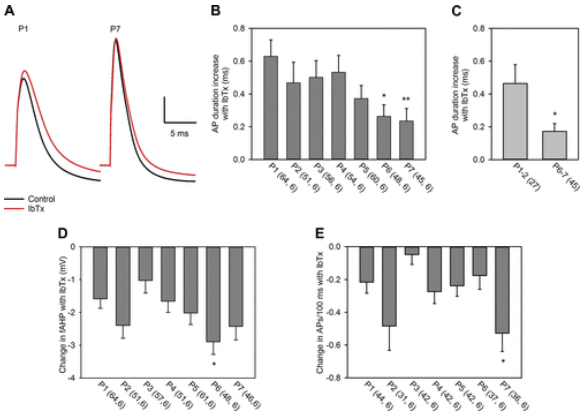

Fig. 5. Iberiotoxin (IbTx) exerts greater effects on the action potential waveform in more mature neurons than in immature neurons. *A*: representative traces comparing the effect of IbTx perfusion (control is in black, IbTx treatment is in red) on action potentials of postnatal day (P)1 and P7 neurons. *B*: average effect of IbTx on action potential (AP) duration. *Significant difference from P1; **significant difference from P1 and P4. (one-way ANOVA on ranks, P = 0.001, Dunn's multiple comparisons, P < 0.05). *C*: average effect of IbTx on action potential duration in P1–P2 and P6–P7 neurons with an initial action potential duration of 2–3 ms (Mann-Whitney rank sum test, P < 0.05). *D*: average magnitude of the effect of IbTx on the fast afterhyperpolarization (fAHP) following a single action potential. *Significant difference from P3 (one-way ANOVA, P < 0.01, Holm-Sidak multiple comparisons, P < 0.01). *E*: average effect of IbTx on the number of action potentials fired in 100 ms for all neurons capable of firing >1 action potentials. *Significant difference from P3 (one-way ANOVA on ranks, P < 0.01, Dunn's multiple comparisons, P < 0.05). For *B*, *D*, and *E*, the first number in parentheses is the number of individual neurons and the second number is the number of rats from which the neurons were obtained. The data in all bar graphs represent means ± SE.

We next examined the effect of IbTx on the fAHP (Fig. 5*D*). While IbTx reduced the magnitude of the fAHP to a greater extent in P6 than in P3 neurons, it is unclear whether this is part of a broader trend, as no significant differences were observed between any other pairs of time points (one-way ANOVA, $P < 0.01$, Holm-Sidak multiple comparisons, $P < 0.01$). Because these recordings were of randomly selected cells in heterogeneous cultures, it is possible that developmental trends were obscured by the variability of the data. To address this, we analyzed the effect of IbTx on fAHP magnitude within groups of cells with similar electrophysiological properties. Action potential data were binned both by initial action potential duration (1–2, 2–3, and 3–4 ms) and by initial magnitude of the fAHP (0–5, 5–10, and 10–15 mV). No age-dependent changes within these groupings were observed (data not shown).

IbTx did not demonstrate a consistent effect on neuronal excitability with a 100-ms stimulation protocol. The mean number of action potentials evoked by a 100-ms depolarization in neurons capable of firing multiple action potentials in the control condition was reduced by 0.05 ± 0.06 in P3 neurons ($n = 42$ cells, 6 animals) and by 0.53 ± 0.11 in P7 neurons ($n = 36$ cells, 6 animals; one way ANOVA, $P < 0.01$, Dunn's multiple comparisons, $P < 0.05$; Fig. 5*E*), but this was the only statistically significant difference and does not necessarily reflect a consistent increase in IbTx effect with age. Age-dependent trends in excitability were somewhat obscured as the population was largely composed of immature, slow-firing neurons.

An important physiological role of BK channels is to enable high-frequency firing (Gu et al. 2007). To examine how the role of BK channels in maintaining action potential firing frequency changes in postnatal development, fast firing hippocampal neurons (initial firing rate >20 Hz with sustained firing throughout the 1-s depolarization) were perfused with 100 nM IbTx while action potential trains (Fig. 6*A*) were evoked by a series of ten 1-s depolarizing pulses from 10 to 100 pA. These fast firing neurons analyzed are likely to be interneurons rather than pyramidal neurons (Jonas et al. 2004; Maccaferri and Lacaille 2003). P1 neurons ($n = 20$ cells, 8 animals) reached maximal firing rates at lower current inputs when compared with P7 neurons ($n = 13$ cells, 4 animals). IbTx had a significant effect on the input-output relationship (two-way ANOVA, $P < 0.001$ for the main effect of IbTx for both ages tested; Fig. 6*B*).

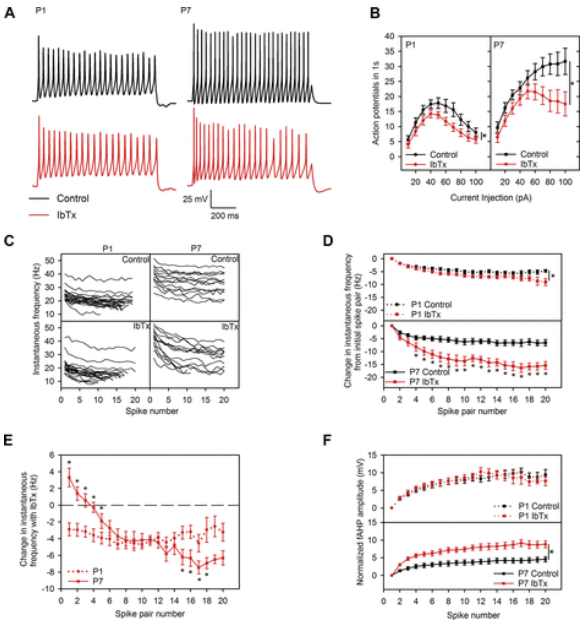

Fig. 6. Iberiotoxin (IbTx) has different effects on the timing of high-frequency action potential firing in postnatal day (P)1 and P7 neurons. *A*: representative traces of 1s action potential trains from P1 and P7 neurons before (black) and after IbTx perfusion (red). *B*: input-output curves for P1 (*left*) and P7 (*right*) neurons without (black

trace) and with IbTx (red trace) for 10–100 pA current injections. *At the end of curves, main effect of IbTx (two-way ANOVA, $P < 0.001$ for the main effect of IbTx). *C*: spike-frequency plots over the first 20 spike pairs for all cells included in the analysis of fast-firing neurons. *D*: average change in instantaneous frequency from the initial instantaneous frequency for the first 20 spike pairs for P1 and P7 fast firing hippocampal neurons before and after IbTx application. *At the end of the P1 curves, main effect of IbTx on successive firing frequency (two-way ANOVA, $P < 0.001$ for the main effect of IbTx). Asterisks comparing individual data points in the P7 curves indicate a significant interaction of IbTx and the spike pair number (two-way ANOVA, $P = 0.002$, Holm-Sidak pairwise comparison, $P < 0.05$). *E*: average effect of IbTx (the difference between instantaneous frequency under IbTx and the instantaneous frequency of the control) on the instantaneous frequency of the first 20 spike pairs. *Significant differences between the effect of IbTx on P1 and P7 neurons at that spike pair (two-way ANOVA, $P < 0.001$, Holm-Sidak multiple comparisons, $P < 0.05$). *F*: average fAHP amplitude following the first 20 action potentials normalized to the amplitude of the first fAHP. *At the end of the P7 curves, main effect of IbTx on fAHP amplitude (two-way ANOVA, $P < 0.001$ for the main effect of IbTx). For all graphs the data represent means ± SE; $n = 20$ neurons from nine rats for P1 and $n = 13$ neurons from four rats for P7.

We analyzed the maximally firing action potential train for each cell. We measured how instantaneous frequency decreased through the first 20 pairs of action potentials, measured as the difference in instantaneous frequency from the initial instantaneous frequency for each spike pair, for trains of action potentials from P1 and P7 neurons before and after IbTx application. Spike frequency plots of the first 20 action potential pairs for all neurons included are illustrated in Fig. 6*C*. Neurons from P1 and P7 rats with and without IbTx showed some degree of spike-frequency adaptation; instantaneous frequencies decreased progressively throughout the action potential train for all conditions (Fig. 6*D*). P1 neurons displayed similar spike-frequency adaptation in the presence and absence of iberiotoxin (Fig. 6*D*, *top*) with the effect of IbTx having a modest effect on instantaneous frequency (two-way ANOVA, $P < 0.001$ for the main effect of IbTx) although no significant differences could be detected for individual spike pairs. In contrast, IbTx perfusion of P7 neurons decreased instantaneous frequencies to a greater degree as action potential firing progressed (interaction of IbTx and spike pair number: $P < 0.001$, two-way ANOVA, Holm-Sidak multiple comparisons, $P < 0.05$), demonstrating that BK channels play a significant role in inhibiting spike frequency adaptation in more mature neurons (Fig. 6*D*, *bottom*).

IbTx-induced changes in instantaneous frequency within the first 20 action potential pairs were analyzed. In P1 neurons ($n = 20$ cells, 9 animals), IbTx decreased action potential firing frequency throughout the action potential train compared with control recordings without IbTx. In P7 neurons ($n = 13$ cells, 4 animals), IbTx significantly increased the instantaneous frequency of the first spike pair and decreased it to an increasingly greater extent as the train progressed. IbTx reduced instantaneous frequency to a greater extent in P1 neurons than in P7 neurons for the first five action potential pairs, while reducing it to a greater extent in cells from P7 animals than in cells from P1 animals for action potential pairs 15–18 (two-way ANOVA, $P < 0.001$, Holm-Sidak multiple comparisons, $P < 0.05$; Fig. 6*E*). Not all cells fired enough action potentials to allow analysis of 20 spike pairs, so statistical power was reduced for later spike pairs. We also tested if IbTx had a different effect on the afterhyperpolarization following each action potential (Fig. 6*F*). IbTx perfusion caused afterhyperpolarizations to reach less negative membrane potentials in P7 fast firing neurons (Fig. 6*F*, *bottom*) but not in P1 fast firing neurons (Fig. 6*F*, *top*).

Among cells that met the defined criteria for fast firing cells, the P7 neurons fired significantly faster (Fig. 6*C*); the initial instantaneous frequency for P1 neurons was 25.13 ± 1.05 Hz versus 39.54 ± 1.92 Hz for P7 neurons (*t* test, $P < 0.01$). To test whether the conclusions drawn from these experiments were appropriate, the analyses were repeated with a smaller subset of the data: the six fastest firing P1 neurons and the six slowest firing P7 neurons. The mean initial instantaneous frequencies of these sets of neurons were not significantly different

and the developmental patterns observed in the full data set were preserved in this subset (data not shown), supporting the conclusion that the differences observed were age dependent.

To further explore differences in the timing and kinetics of BK channels across the first postnatal week, we performed whole cell voltage-clamp recordings of total potassium currents in cultured neurons. Samples of whole cell potassium currents are shown in Fig. 7*A* both with and without IbTx treatment. We found that in P1 neurons, IbTx decreased the maximum rise slope of the current evoked by a step in the membrane potential from −90 mV to +50 mV (depicted in Fig. 7*B*) by 12.01 ± 1.91% (*n* = 32 cells, 4 animals) and by 1.94 ± 1.70% in P7 neurons (*n* = 39 cells, 5 animals; Mann-Whitney rank sum test, *P* < 0.001; Fig. 7*C*). This demonstrated that BK channels have a larger role in total potassium currents at P1 than at P7.

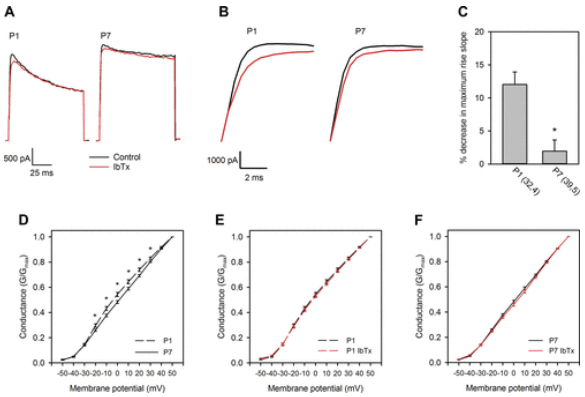

Fig. 7. Large-conductance calcium-activated potassium (BK) channels contribute to more to fast onset potassium currents in postnatal day (P)1 neurons than in P7 neurons. *A*: representative traces of potassium currents evoked by 100-ms depolarizations from −90 mV to 50 mV in hippocampal neurons cultured from P1 and P7 rats. The untreated control is shown in black; the iberiotoxin (IbTx)-treated recording is shown in red. *B*: the rise slope of the representative currents from *panel A* illustrating the effect of IbTx on the rate of current onset. *C*: average percent reduction in the maximum rise slope of whole cells potassium currents evoked by a membrane potential step from −90 mV to +50 mV in P1 and P7 neurons. *Significant difference between P1 and P7 (Mann-Whitney rank sum test, *P* < 0.001). *D*: relative conductance plots (G/G_{max}) for whole potassium currents in hippocampal neurons cultured from P1 and P7 rats. *Significant difference between P1 and P7 at each conductance (three-way ANOVA, *P* < 0.001 for the interaction of age and membrane potential. Holm-Sidak pairwise comparisons, *P* > 0.01). *E*: relative conductance plots of total potassium currents and IbTx-treated potassium currents in P1 neurons. *F*: relative conductance plots of total potassium currents and IbTx-treated potassium currents in P7 neurons. For *C*–*F*, *n* = 34 cells from 4 animals for P1 and *n* = 39 cells from 5 animals for P7; data represent means ± SE.

The relative conductance of total potassium currents with and without IbTx treatment in P1 and P7 neurons at membrane potentials from −50 mV to 50 mV is illustrated in Fig. 7, *D*–*F*. From P1 to P7 the voltage-conductance curve is shifted to the right, which is similar in trend but smaller in magnitude than the difference in voltage dependence when comparing isolated currents through STREX and ZERO channels expressed in HEK293 cells (Chen et al. 2005). The small size of the voltage-dependent shift in our data is likely due to the fact that we measured total potassium current, not just BK current and the shift from STREX to ZERO may not be complete at P7 (Fig. 7*D*; three-way ANOVA with membrane potential, age, and IbTx treatment as variables, *P* < 0.001 for the interaction of membrane potential and age, pairwise comparisons significant for V_m = −20 to +30 mV, *P* < 0.05, Holm-Sidak method). Treatment with IbTx shifted the voltage-conductance relationship slightly to the right in both P1 and P7 neurons (Fig. 7, *E* and *F*; three-way ANOVA, *P* < 0.03 for the main of effect of IbTx).

DISCUSSION

We found that excitability of hippocampal neurons increases through the first postnatal week, with the action potential waveform increasing in amplitude and decreasing in duration while neurons become capable of firing more successive action potentials before entering depolarizing block. This was true in neurons acutely isolated from different age rats and allowed to remain in culture overnight as well as in neurons in acute hippocampal slices taken from different aged rats. Our data also demonstrate that as development progresses and BK channel expression increases, the contribution of BK channels to the repolarization of single action potentials decreases and BK channels contribute less to fast onset potassium currents. At the same time, there is a shift in the timing of the effect of BK channel blockade in high-frequency firing, such that BK currents appear to contribute to spike-frequency adaptation and afterhyperpolarizations in P7 but not P1 neurons. IbTx-sensitive BK channel contribution to the total potassium current is larger in neurons isolated from P1 rats than in neurons isolated from P7 rats and the difference in the voltage-conductance relationships between the two populations demonstrates a developmental shift of the voltage dependence to more positive potentials as the neurons mature.

Our findings on the increases in intrinsic excitability and changes in the action potential waveform through early development are consistent with previous reports in other neuronal populations (Gao and Ziskind-Conhaim 1998; Goldberg et al. 2011; Kinnischtzke et al. 2012; McCormick and Prince 1987). Prior data on changes in BK channel activity in this time period are limited, but one report found that channel density increases from postnatal *day 1* to *day 28* and expression studies show that BK mRNA expression increases sharply throughout the central nervous system during the first postnatal week (Kang et al. 1996; MacDonald et al. 2006). Our Western blot analysis of steady-state BK protein expression are in agreement with the mRNA studies. While it may appear contradictory to observe greater contributions of BK channels to single action potentials in early development, this is sufficiently explained by a shift from fast activating BK channel variants to slow-activating variants. Macdonald et al. report a shift in the dominant hippocampal BK isoform from STREX, a more calcium-sensitive, faster acting variant to the slower ZERO isoform, a variant that may have too long of an activation time to influence the waveform of a single action potential (Chen et al. 2005; MacDonald et al. 2006; Xie and McCobb 1998). We show that a component of the total potassium current in neurons from P1 rats opens more readily at lower voltages, which may be due to the inclusion of the STREX insert in BK channels. The change in timing of IbTx effects on prolonged firing observed in this report may also be explained by the transition of the dominant BK α-subunit isoform.

β-Subunit association can also affect the BK channel's activation timing. The β4-subunit, a neuronally expressed β-subunit, increases the calcium sensitivity but also slows the kinetics of the BK channel such that it would not participate in repolarization of a single action potential (Behrens et al. 2000). Levels of β4-subunit mRNA (Kcnmb4) increase in the hippocampus with postnatal development making changes in beta subunit association another avenue to explore in examining postnatal changes in BK channels activity. However, it is unlikely that this is the source of the changes that we observed as we used the BK antagonist IbTx to examine BK channel activity; BK channels associated with the β4-subunit are reportedly insensitive to blockade with IbTx as well as charybdotoxin (Meera et al. 2000).

The early postnatal period is notable for being a period of heightened seizure susceptibility (Rakhade and Jensen 2009). This is likely due to many reasons as the brain undergoes extensive developmental changes after birth. These reasons may include immature patterns of BK channel expression as described here. This is supported by findings that BK channel dysfunction can be causative in epilepsy. Administration of the BK channel antagonist paxilline reduces the incidence and duration of seizures in immature mice (Sheehan et al. 2009). One mutation in the intracellular RCK domain of the BK channel D343G has been identified in clinical settings as causative in epilepsy and paroxysmal dyskinesia (Du et al. 2005). The effect of this mutation is to shift the channel's

activation profile to the left, similar to the effect of inclusion of the STREX insert (Du et al. 2005; Yang et al. 2010). The STREX isoform also contributes to burst firing in hippocampal neurons (Bell et al. 2010). This suggests that the early predominance of the STREX isoform may increase seizure susceptibility. The β4-subunit of the BK channel increases with postnatal development and deletion of the β4-subunit results in seizures (Brenner et al. 2005). Thus lower expression of the β4-subunit in early development may also contribute to seizure formation. Additionally, lower overall expression of the BK channel itself in interneurons may contribute to epilepsy as BK channels permit for high-frequency firing, a hallmark of interneuron activity that is necessary to regulate coordinated network activity in the hippocampus.

Understanding the implications of changes in BK expression and activity involves understanding these trends in the context of specific cellular subpopulations; the hippocampus comprises a diverse population of interneurons with varying roles in maintaining proper hippocampal excitability (for review see Pelkey et al. 2017). Changes in the excitability of a cell type could have differential effects on circuit excitability depending on the role of that neuronal type in controlling the circuit excitability. Optogenetic and chemogenetic experiments have demonstrated that activating interneurons that directly inhibit pyramidal neurons (such as the parvalbumin and somatostatin expressing interneurons) can inhibit seizures, while activating cells that inhibit this first class of cells (such as VIP-expressing interneurons) can potentiate excitatory transmission in the hippocampus (Călin et al. 2018; Karnani et al. 2016). The present study did not used labeled neurons so that only biophysical properties were available for distinguishing between cells. While some information about cell identity can be gleaned from their firing properties, that alone does not reliably differentiate cell populations (Wheeler et al. 2015). The use of firing properties alone is further confounded by the fact that action excitability changes rapidly in the early postnatal period. This work should be followed up by efforts to characterize trends in BK channel expression and activity in identified hippocampal neurons. Parvalbumin and somatostatin expressing interneurons are of particular interest since previous studies have demonstrated that activity in these interneurons may play a role in seizure activity (Călin et al. 2018; Sessolo et al. 2015; Yekhlef et al. 2015). The immature properties and expression patterns of BK channels in these neurons may contribute to early postnatal seizure susceptibility.

GRANTS

This work has been funded by the Marquette University Committee in Research and the Marquette University Department of Biological Sciences.

DISCLOSURES

No conflicts of interest, financial or otherwise, are declared by the authors.

AUTHOR CONTRIBUTIONS

M.S.H. and M.M. conceived and designed research; M.S.H. performed experiments; M.S.H. and M.M. analyzed data; M.S.H. and M.M. interpreted results of experiments; M.S.H. prepared figures; M.S.H. drafted manuscript; M.S.H. and M.M. edited and revised manuscript; M.S.H. and M.M. approved final version of manuscript.

ACKNOWLEDGMENTS

The authors thank an undergraduate student, Alexis Monical, for her role in the initial data collection for this study. The authors also thank Dr. Deanna Arble for constructive feedback during the revision process.

References

Aika Y, Ren JQ, Kosaka K, Kosaka T. Quantitative analysis of GABA-like-immunoreactive and parvalbumin-containing neurons in the CA1 region of the rat hippocampus using a stereological method, the disector. ***Exp Brain Res*** 99: 267–276, 1994. doi:10.1007/BF00239593.

Banker GA, Cowan WM. Further observations on hippocampal neurons in dispersed cell culture. ***J Comp Neurol*** 187: 469–493, 1979. doi:10.1002/cne.901870302.

Behrens R, Nolting A, Reimann F, Schwarz M, Waldschütz R, Pongs O. hKCNMB3 and hKCNMB4, cloning and characterization of two members of the large-conductance calcium-activated potassium channel β subunit family. ***FEBS Lett*** 474: 99–106, 2000. doi:10.1016/S0014-5793(00)01584-2.

Bell TJ, Miyashiro KY, Sul JY, Buckley PT, Lee MT, McCullough R, Jochems J, Kim J, Cantor CR, Parsons TD, Eberwine JH. Intron retention facilitates splice variant diversity in calcium-activated big potassium channel populations. ***Proc Natl Acad Sci USA*** 107: 21152–21157, 2010. doi:10.1073/pnas.1015264107.

Brenner R, Chen QH, Vilaythong A, Toney GM, Noebels JL, Aldrich RW. BK channel beta4 subunit reduces dentate gyrus excitability and protects against temporal lobe seizures. ***Nat Neurosci*** 8: 1752–1759, 2005. doi:10.1038/nn1573.

Călin A, Stancu M, Zagrean AM, Jefferys JG, Ilie AS, Akerman CJ. Chemogenetic recruitment of specific interneurons suppresses seizure activity. ***Front Cell Neurosci*** 12: 293, 2018. doi:10.3389/fncel.2018.00293.

Chen L, Tian L, MacDonald SH, McClafferty H, Hammond MS, Huibant JM, Ruth P, Knaus HG, Shipston MJ. Functionally diverse complement of large conductance calcium- and voltage-activated potassium channel (BK) alpha-subunits generated from a single site of splicing. ***J Biol Chem*** 280: 33599–33609, 2005. doi:10.1074/jbc.M505383200.

Cline HT. Dendritic arbor development and synaptogenesis. ***Curr Opin Neurobiol*** 11: 118–126, 2001. doi:10.1016/S0959-4388(00)00182-3.

Du W, Bautista JF, Yang H, Diez-Sampedro A, You SA, Wang L, Kotagal P, Lüders HO, Shi J, Cui J, Richerson GB, Wang QK. Calcium-sensitive potassium channelopathy in human epilepsy and paroxysmal movement disorder. ***Nat Genet*** 37: 733–738, 2005. doi:10.1038/ng1585.

Dzhala VI, Staley KJ. Excitatory actions of endogenously released GABA contribute to initiation of ictal epileptiform activity in the developing hippocampus. ***J Neurosci*** 23: 1840–1846, 2003. doi:10.1523/JNEUROSCI.23-05-01840.2003.

Fridén M, Ducrozet F, Middleton B, Antonsson M, Bredberg U, Hammarlund-Udenaes M. Development of a high-throughput brain slice method for studying drug distribution in the central nervous system. ***Drug Metab Dispos*** 37: 1226–1233, 2009. doi:10.1124/dmd.108.026377.

Galvez A, Gimenez-Gallego G, Reuben JP, Roy-Contancin L, Feigenbaum P, Kaczorowski GJ, Garcia ML. Purification and characterization of a unique, potent, peptidyl probe for the high conductance calcium-activated potassium channel from venom of the scorpion Buthus tamulus. ***J Biol Chem*** 265: 11083–11090, 1990.

Gao BX, Ziskind-Conhaim L. Development of ionic currents underlying changes in action potential waveforms in rat spinal motoneurons. ***J Neurophysiol*** 80: 3047–3061, 1998. doi:10.1152/jn.1998.80.6.3047.

Goldberg EM, Jeong HY, Kruglikov I, Tremblay R, Lazarenko RM, Rudy B. Rapid developmental maturation of neocortical FS cell intrinsic excitability. ***Cereb Cortex*** 21: 666–682, 2011. doi:10.1093/cercor/bhq138.

Gómez-Di Cesare CM, Smith KL, Rice FL, Swann JW. Axonal remodeling during postnatal maturation of CA3 hippocampal pyramidal neurons. ***J Comp Neurol*** 384: 165–180, 1997. doi:10.1002/(SICI)1096-9861(19970728)384:2<165:AID-CNE1>3.0.CO;2-#.

Gu N, Vervaeke K, Storm JF. BK potassium channels facilitate high-frequency firing and cause early spike frequency adaptation in rat CA1 hippocampal pyramidal cells. ***J Physiol*** 580: 859–882, 2007. doi:10.1113/jphysiol.2006.126367.

Huttenlocher PR, Dabholkar AS. Regional differences in synaptogenesis in human cerebral cortex. ***J Comp Neurol*** 387: 167–178, 1997. doi:10.1002/(SICI)1096-9861(19971020)387:2<167:AID-CNE1>3.0.CO;2-Z.

Jaffe DB, Wang B, Brenner R. Shaping of action potentials by type I and type II large-conductance Ca^{2+}-activated K^+ channels. ***Neuroscience*** 192: 205–218, 2011. doi:10.1016/j.neuroscience.2011.06.028.

Jonas P, Bischofberger J, Fricker D, Miles R. Interneuron Diversity series: Fast in, fast out—temporal and spatial signal processing in hippocampal interneurons. ***Trends Neurosci*** 27: 30–40, 2004. doi:10.1016/j.tins.2003.10.010.

Kang J, Huguenard JR, Prince D. Development of BK channels in neocortical pyramidal neurons. ***J Neurophysiol*** 76: 18–198, 1996. doi:10.1152/jn.1996.76.1.188.

Karnani MM, Jackson J, Ayzenshtat I, Hamzehei Sichani A, Manoocheri K, Kim S, Yuste R. Opening holes in the blanket of inhibition: localized lateral disinhibition by vip interneurons. ***J Neurosci*** 36: 3471–3480, 2016. doi:10.1523/JNEUROSCI.3646-15.2016.

Kinnischtzke AK, Sewall AM, Berkepile JM, Fanselow EE. Postnatal maturation of somatostatin-expressing inhibitory cells in the somatosensory cortex of GIN mice. ***Front Neural Circuits*** 6: 33, 2012. doi:10.3389/fncir.2012.00033.

Koschak A, Koch RO, Liu J, Kaczorowski GJ, Reinhart PH, Garcia ML, Knaus H-G. [^{125}I]Iberiotoxin-D19Y/Y36F, the first selective, high specific activity radioligand for high-conductance calcium-activated potassium channels. ***Biochemistry*** 36: 1943–1952, 1997. doi:10.1021/bi962074m.

Kumar SS, Bacci A, Kharazia V, Huguenard JR. A developmental switch of AMPA receptor subunits in neocortical pyramidal neurons. ***J Neurosci*** 22: 3005–3015, 2002. doi:10.1523/JNEUROSCI.22-08-03005.2002.

Maccaferri G, Lacaille JC. Interneuron Diversity series: Hippocampal interneuron classifications—making things as simple as possible, not simpler. ***Trends Neurosci*** 26: 564–571, 2003. doi:10.1016/j.tins.2003.08.002.

MacDonald SH, Ruth P, Knaus HG, Shipston MJ. Increased large conductance calcium-activated potassium (BK) channel expression accompanied by STREX variant downregulation in the developing mouse CNS. ***BMC Dev Biol*** 6: 37, 2006. doi:10.1186/1471-213X-6-37.

Magistretti J, Mantegazza M, Guatteo E, Wanke E. Action potentials recorded with patch-clamp amplifiers: are they genuine? ***Trends Neurosci*** 19: 530–534, 1996. doi:10.1016/S0166-2236(96)40004-2.

McCormick DA, Prince DA. Post-natal development of electrophysiological properties of rat cerebral cortical pyramidal neurones. ***J Physiol*** 393: 743–762, 1987. doi:10.1113/jphysiol.1987.sp016851.

Meera P, Wallner M, Toro L. A neuronal β subunit (KCNMB4) makes the large conductance, voltage- and Ca^{2+}-activated K^+ channel resistant to charybdotoxin and iberiotoxin. ***Proc Natl Acad Sci USA*** 97: 5562–5567, 2000. doi:10.1073/pnas.100118597.

Misonou H, Menegola M, Buchwalder L, Park EW, Meredith A, Rhodes KJ, Aldrich RW, Trimmer JS. Immunolocalization of the Ca^{2+}-activated K^+ channel Slo1 in axons and nerve terminals of mammalian brain and cultured neurons. ***J Comp Neurol*** 496: 289–302, 2006. doi:10.1002/cne.20931.

Mynlieff M. Dissociation of postnatal hippocampal neurons for short term culture. ***J Neurosci Methods*** 73: 35–44, 1997. doi:10.1016/S0165-0270(96)02209-1.

Mynlieff M. Identification of different putative neuronal subtypes in cultures of the superior region of the hippocampus using electrophysiological parameters. ***Neuroscience*** 93: 479–486, 1999. doi:10.1016/S0306-4522(99)00153-0.

Pelkey KA, Chittajallu R, Craig MT, Tricoire L, Wester JC, McBain CJ. Hippocampal gabaergic inhibitory interneurons. ***Physiol Rev*** 97: 1619–1747, 2017. doi:10.1152/physrev.00007.2017.

Picken Bahrey HL, Moody WJ. Early development of voltage-gated ion currents and firing properties in neurons of the mouse cerebral cortex. ***J Neurophysiol*** 89: 1761–1773, 2003. doi:10.1152/jn.00972.2002.

Rakhade SN, Jensen FE. Epileptogenesis in the immature brain: emerging mechanisms. ***Nat Rev Neurol*** 5: 380–391, 2009. doi:10.1038/nrneurol.2009.80.

Sessolo M, Marcon I, Bovetti S, Losi G, Cammarota M, Ratto GM, Fellin T, Carmignoto G. Parvalbumin-positive inhibitory interneurons oppose propagation but favor generation of focal epileptiform activity. ***J Neurosci*** 35: 9544–9557, 2015. doi:10.1523/JNEUROSCI.5117-14.2015.

Sheehan JJ, Benedetti BL, Barth AL. Anticonvulsant effects of the BK-channel antagonist paxilline. ***Epilepsia*** 50: 711–720, 2009. doi:10.1111/j.1528-1167.2008.01888.x.

Szczurowska E, Mareš P. NMDA and AMPA receptors: development and status epilepticus. ***Physiol Res*** 62, Suppl 1: S21–S38, 2013.

Wheeler DW, White CM, Rees CL, Komendantov AO, Hamilton DJ, Ascoli GA. Hippocampome.org: a knowledge base of neuron types in the rodent hippocampus. ***eLife*** 4: e09960, 2015. doi:10.7554/eLife.09960.

Xie J, McCobb DP. Control of alternative splicing of potassium channels by stress hormones. ***Science*** 280: 443–446, 1998. doi:10.1126/science.280.5362.443.

Yang J, Krishnamoorthy G, Saxena A, Zhang G, Shi J, Yang H, Delaloye K, Sept D, Cui J. An epilepsy/dyskinesia-associated mutation enhances BK channel activation by potentiating Ca^{2+} sensing. ***Neuron*** 66: 871–883, 2010. doi:10.1016/j.neuron.2010.05.009.

Yekhlef L, Breschi GL, Lagostena L, Russo G, Taverna S. Selective activation of parvalbumin- or somatostatin-expressing interneurons triggers epileptic seizurelike activity in mouse medial entorhinal cortex. ***J Neurophysiol*** 113: 1616–1630, 2015. doi:10.1152/jn.00841.2014.

Zhou X, Wulfsen I, Korth M, McClafferty H, Lukowski R, Shipston MJ, Ruth P, Dobrev D, Wieland T. Palmitoylation and membrane association of the stress axis regulated insert (STREX) controls BK channel regulation by protein kinase C. ***J Biol Chem*** 287: 32161–32171, 2012. doi:10.1074/jbc.M112.386359.

Zhou XB, Wulfsen I, Utku E, Sausbier U, Sausbier M, Wieland T, Ruth P, Korth M. Dual role of protein kinase C on BK channel regulation. ***Proc Natl Acad Sci USA*** 107: 8005–8010, 2010. doi:10.1073/pnas.0912029107.